Inorganic Chemistry
Article

Inorg. Chem. **2010**, *49*, 3489–3500 **3489**
DOI: 10.1021/ic100103k

A Series of New Manganese(II) Sulfonate-Arsonates with 2D Layer, 1D Chain, and 0D Clusters Structures

Fei-Yan Yi,[†,‡] Qi-Pu Lin,[†,‡] Tian-Hua Zhou,[†] and Jiang-Gao Mao*[,†]

[†]*State Key Laboratory of Structure Chemistry, Fujian Institute of Research on the Structure of Matter, Chinese Academy of Sciences, Fuzhou 350002, P.R. China, and* [‡]*Graduate University of Chinese Academy of Sciences, Beijing 100039, P.R. China*

Received January 17, 2010

Hydrothermal reactions of manganese(II) salts with *o*-sulfophenylarsonic acid (*o*-$HO_3S-C_6H_4-AsO_3H_2$, H_3L) afforded $Mn_3(L)_2(H_2O)_3\cdot H_2O$ (**1**) with a layered structure. When 1,10-phenanthroline (phen), 2,2′-bipyridine (bipy), and 2,2′:6′,2″-terpyridine (terpy) were used as auxiliary chelating ligands, a series of mixed-ligand manganese(II) sulfonate-arsonates with lower dimensional structures, namely, $[Mn(HL)(phen)_2]_2\cdot 8.5H_2O$ (**2**), $Mn(HL)(phen)_2(H_2O)\cdot 2H_2O$ (**3**), $[Mn(HL)(bipy)_2][Mn(H_2L)(bipy)_2](ClO_4)\cdot 3H_2O$ (**4**), [Mn(HL)(phen)][Mn(HL)-(phen)(H_2O)] (**5**), $[Mn_2(HL)(phen)_4(H_2O)](ClO_4)_2\cdot 4H_2O$ (**6**), $[Mn_2(HL)(phen)_4(H_2O)](ClO_4)_2\cdot H_2O$ (**7**), $Mn_2(HL)_2$-$(bipy)_3(H_2O)\cdot H_2O$ (**8**), $[Mn(HL)(terpy)]_2$ (**9**), $Mn_7(OH)_2(L)_4(phen)_8\cdot 10H_2O\cdot$phen (**10**), and Mn(HL)(bipy)-$(H_2O)\cdot 2H_2O$ (**11**) have been obtained. **2**−**4** are mononuclear (**4** contains two different mononuclear cluster units) whereas **5**−**9** feature three types of isolated dinuclear cluster units in which the two Mn^{2+} ions are bridged by one or two sulfonate-arsonate ligands. **10** exhibits an interesting heptanuclear cluster in which the Mn^{2+} centers are bridged by arsonate, sulfonate groups and hydroxyl anions. **11** features a one-dimensional (1D) chain in which two neighboring Mn^{2+} centers are bridged by an arsonate group of a sulfonate-arsonate ligand. Magnetic measurements indicate that **1** exhibits an unprecedented spin topology and behaves as a homospin ferrimagnet whereas **2**−**4** are essentially paramagnetic. **5**−**9** and **11** are weakly antiferromagnetic.

Introduction

The chemistry of metal phosphonates has been an active research area in recent years because of its potential applications in the areas of catalysis, ion exchange, proton conductivity, intercalation chemistry, photochemistry, and materials chemistry.[1,2] Most of metal phosphonates display a layered structure in which the metal centers are bridged by the phosphonate groups, although a variety of one-dimensional (1D) chains and porous three-dimensional (3D) networks have also been reported.[3] Metal phosphonates containing a molecular cluster unit have been also isolated.[4−10] Metal arsonates are expected to display a similar structural chemistry to those of metal phosphonates, but the larger ionic

*To whom correspondence should be addressed. E-mail: mjg@fjirsm.ac.cn.

(1) (a) Clearfield, A. *Metal phosphonate chemistry in Progress in Inorganic Chemistry*; Karlin, K. D., Ed.; John Wiley & Sons: New York, 1998; Vol. *47*, pp 371−510 (and references therein). (b) Mao, J.-G. *Coord. Chem. Rev.* **2007**, *251*, 1493–1520. (c) Matczak-Jon, E.; Videnova-Adrabinska, V. *Coord. Chem. Rev.* **2005**, *249*, 2458–2488.

(2) (a) Cheetham, A. K.; Ferey, G.; Loiseau, T. *Angew. Chem., Int. Ed.* **1999**, *38*, 3268–3292. (b) Zhu, J.; Bu, X.; Feng, P.; Stucky, G. D. *J. Am. Chem. Soc.* **2000**, *122*, 11563–11564. (c) Rao, C. N. R.; Natarajan, S.; Vaidhyanathan, R. *Angew. Chem., Int. Ed.* **2004**, *43*, 1466–1496.

(3) (a) Maeda, K. *Microporous Mesoporous Mater.* **2004**, *73*, 47−55 (and references therein). (b) Kubicek, V.; Kotek, J.; Hermann, P.; Lukes, I. *Eur. J. Inorg. Chem.* **2007**, 333–344. (c) Tang, S.-F.; Song, J.-L.; Li, X.-L.; Mao, J.-G. *Cryst. Growth Des.* **2007**, *7*, 360–366. (d) Konar, S.; Zon, J.; Prosvirin, A. V.; Dunbar, K. R.; Clearfield, A. *Inorg. Chem.* **2007**, *46*, 5229–5236.

(4) (a) Comby, S.; Scopelliti, R.; Imbert, D.; Charbonniere, L.; Ziessel, R.; Bunzli, J.-C. G. *Inorg. Chem.* **2006**, *45*, 3158–3160. (b) Du, Z.-Y.; Xu, H.-B.; Mao, J.-G. *Inorg. Chem.* **2006**, *45*, 9780–9788. (c) Cao, D.-K.; Xiao, J.; Tong, J.-W.; Li, Y.-Z.; Zheng, L.-M. *Inorg. Chem.* **2007**, *46*, 428–436. (d) Bao, S.-S.; Ma, L.-F.; Wang, Y.; Fang, L.; Zhu, C.-J.; Li, Y.-Z.; Zheng, L.-M. *Chem.—Eur. J.* **2007**, *13*, 2333–2343.

(5) (a) Walawalker, M. G.; Roesky, H. W.; Murugavel, R. *Acc. Chem. Res.* **1999**, *32*, 117−126 (and references therein). (b) Konar, S.; Clearfield, A. *Inorg. Chem.* **2008**, *47*, 5573–5579. (c) Konar, S.; Clearfield, A. *Inorg. Chem.* (*Communication*) **2008**, *47*, 3489–3491.

(6) (a) Dumas, E.; Sassoye, C.; Smith, K. D.; Sevov, S. C. *Inorg. Chem.* **2002**, *41*, 4029–4032. (b) Konar, S.; Bhuvanesh, N.; Clearfield, A. *J. Am. Chem. Soc.* **2006**, *128*, 9604–9605. (c) Yao, H. C.; Wang, J.-J.; Ma, Y.-S.; Waldmann, O.; Du, W.-X.; Song, Y.; Li, Y.-Z.; Zheng, L.-M.; Decurtins, S.; Xin, X.-Q. *Chem. Commun.* **2006**, 1745–1747. (d) Yao, H.-C.; Li, Y.-Z.; Zheng, L.-M.; Xin, X.-Q. *Inorg. Chim. Acta* **2005**, *358*, 2523–2529. (e) Yao, H.-C.; Li, Y.-Z.; Song, Y.; Ma, Y.-S.; Zheng, L.-M.; Xin, X.-Q. *Inorg. Chem.* **2006**, *45*, 59–65.

(7) (a) Chandrasekhar, V.; Kingsley, S. *Angew. Chem., Int. Ed.* **2000**, *39*, 2320–2322. (b) Yang, Y.; Pinkas, J.; Noltemeyer, M.; Schmidt, H.-G.; Roesky, H. W. *Angew. Chem., Int. Ed.* **1999**, *38*, 664–666. (c) Chandrasekhar, V.; Sasikumar, P.; Boomishankar, R.; Anantharaman, G. *Inorg. Chem.* **2006**, *45*, 3344–3351. (d) Lei, C.; Mao, J.-G.; Sun, Y.-Q.; Zeng, H.-Y.; Clearfield, A. *Inorg. Chem.* **2003**, *42*, 6157–6159. (e) Yang, B.-P.; Mao, J.-G.; Sun, Y.-Q.; Zhao, H.-H.; Clearfield, A. *Eur. J. Inorg. Chem.* **2003**, 4211–4217. (f) Cao, D.-K.; Li, Y.-Z.; Zheng, L.-M. *Inorg. Chem.* **2005**, *44*, 2984–2985. (g) Du, Z.-Y.; Xu, H.-B.; Mao, J.-G. *Inorg. Chem.* **2006**, *45*, 6424–6430.

Published on Web 03/03/2010

radius of As(V) compared to P(V) could lead to some different architectures with different physical properties. So far, reports on metal organo arsonates are still limited.[11−17] A variety of polyoxometalate (POM) clusters based on vanadium, molybdenum, and tungsten arsonates were reported.[11−13] A few organo oxo tin clusters with organo arsonates were recently synthesized solvothermally by Ma's group.[16] In the presence of an auxiliary ligand such as 5-sulfoisophthalic acid monosodium salt (NaH_2SIP) or 1,3,5-benzenetricarboxylic acid (H_3BTC)), three novel mixed-ligand lead(II) carcoxylate-arsonates with 1D to 3D structures have been isolated by our group.[17a] When the second metal linker was changed to the N-donor chelating ligands such as phen or bipy, metal arsonates with lower dimensional structures were successfully isolated.[17b]

Scheme 1. Synthetic Route for Compounds **1**−**11**

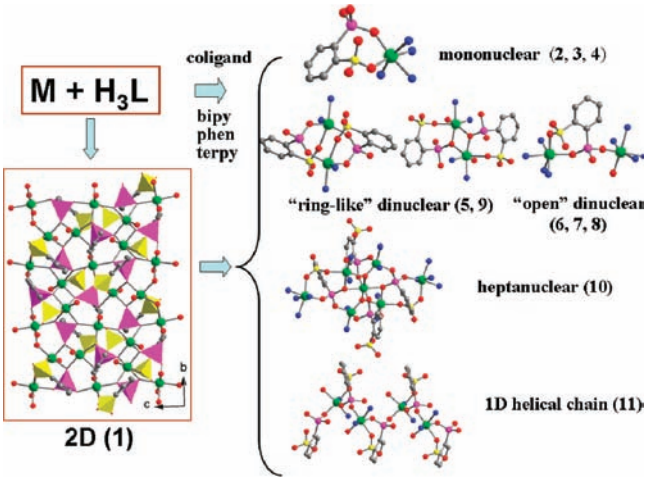

Manganese-based coordination compounds have received considerable interest in the fields of supramolecular chemistry, crystal engineering, and materials chemistry, because of not only their remarkable magnetochemical properties[18] but also their relevance in biochemistry.[19] So far, reports on manganese(II) phenylarsonates with polynuclear cluster units are still relatively scarce.[17b] The design of polynuclear metal compounds remains a great challenge. One possible route to design metal arsonates with low dimensional structures such as isolated clusters and 1D chains is to attack a weak coordination sulfonate group to the phenylarsonic acid, such as *o*-$HO_3S-C_6H_4-AsO_3H_2$, and introducing a suitable auxiliary ligand such as bipy, phen, and 2,2′:6′,2″-terpyridine (terpy). A weak-coordination sulfonate group attached on an arsonic acid can not only increase the solubility of the metal arsonates because of its acidic nature and hydrogen bonds formation but also provide a larger steric hindrance. On the other hand, the coordination of the auxiliary chelating ligands reduces the coordination sites of the metal centers; hence, the arsonate ligand can only form a variety of small aggregations with fewer metal ions. Such method has been proven effective by our work.[7g,20] Guided by this idea, first $Mn_3(L)_2(H_2O)_3\cdot H_2O$ (**1**) with a layered structure was isolated. By using phen, bipy, and terpy as the auxiliary chelating ligands, a series of novel manganese(II) sulfonate-arsonates with zero-dimensional (0D) and 1D structures have been synthesized subsequently, namely, $[Mn(HL)(phen)_2]_2\cdot 8.5H_2O$ (**2**), $Mn(HL)(phen)_2(H_2O)\cdot 2H_2O$ (**3**), $[Mn(HL)(bipy)_2][Mn(H_2L)(bipy)_2](ClO_4)\cdot 3H_2O$ (**4**), $[Mn(HL)(phen)][Mn(HL)(phen)(H_2O)]$ (**5**), $[Mn_2(HL)(phen)_4(H_2O)](ClO_4)_2\cdot 4H_2O$ (**6**), $[Mn_2(HL)(phen)_4(H_2O)](ClO_4)_2\cdot H_2O$ (**7**), $Mn_2(HL)_2(bipy)_3(H_2O)\cdot H_2O$ (**8**), $[Mn(HL)(terpy)]_2$ (**9**), $Mn_7(OH)_2(L)_4(phen)_8\cdot 10H_2O\cdot$phen (**10**), and $Mn(HL)(bipy)(H_2O)\cdot 2H_2O$ (**11**) (Scheme 1). **2**−**4** are mononuclear (**4** contains two different mononuclear cluster units) whereas **5**−**9** feature three types of dinuclear cluster units in which neighboring two Mn^{2+} ions are bridged by one or two

(8) (a) Langley, S. J.; Helliwell, M.; Sessoli, R.; Rosa, P.; Wernsdorfer, W.; Winpenny, R. E. P. *Chem. Commun.* **2005**, 5029–5031. (b) Brechin, E. K.; Coxall, R. A.; Parkin, A.; Parsons, S.; Tasker, P. A.; Winpenny, R. E. P. *Angew. Chem., Int. Ed.* **2001**, *40*, 2700–2703. (c) Tolis, E. I.; Helliwell, M.; Langley, S.; Raftery, J.; Winpenny, R. E. P. *Angew. Chem., Int. Ed.* **2003**, *42*, 3804–3808. (d) Tolis, E. I.; Engelhardt, L. P.; Mason, P. V.; Rajaraman, G.; Kindo, K.; Luban, M.; Matsuo, A.; Nojiri, H.; Raftery, J.; Schröder, C.; Timco, G. A.; Tuna, F.; Wernsdorfer, W.; Winpenny, R. E. P. *Chem.—Eur. J.* **2006**, *12*, 8961–8968.

(9) (a) Langley, S.; Helliwell, M.; Sessoli, R.; Teat, S. J.; Winpenny, R. E. P. *Inorg. Chem.* **2008**, *47*, 497–507. (b) Breeze, B. A.; Shanmugam, M.; Tuna, F.; Winpenny, R. E. P. *Chem. Commun.* **2007**, 5185–5187. (c) Baskar, V.; Shanmugam, M.; Carolina Sañudo, E.; Shanmugam, M.; Collison, D.; McInnes, E. J. L.; Wei, Q.; Winpenny, R. E. P. *Chem. Commun.* **2007**, 37–39.

(10) (a) Maheswaran, S.; Chastanet, G.; Teat, S. J.; Mallah, T.; Sessoli, R.; Wernsdorfer, W.; Winpenny, R. E. P. *Angew. Chem., Int. Ed.* **2005**, *44*, 5044–5048. (b) Shanmugam, M.; Chastanet, G.; Mallah, T.; Sessoli, R.; Teat, S. J.; Timco, G. A.; Winpenny, R. E. P. *Chem.—Eur. J.* **2006**, *12*, 8777–8785. (c) Shanmugam, M.; Shanmugam, M.; Chastanet, G.; Sessoli, R.; Mallah, T.; Wernsdorfe, W.; Winpenny, R. E. P. *J. Mater. Chem.* **2006**, *16*, 2576–2578.

(11) (a) Burkholder, E.; Zubieta, J. *Inorg. Chim. Acta* **2004**, *357*, 301–304. (b) Burkholder, E.; Wright, E.; Golub, V.; O'Connor, C. J.; Zubieta, J. *Inorg. Chem.* **2003**, *42*, 7460–7471. (c) Barkigia, K. M.; Rajkovic-Blazer, L. M.; Pope, M. T.; Quicksall, C. O. *Inorg. Chem.* **1981**, *20*, 3318–3323. (d) Johnson, B. J. S.; Geers, S. A.; Brennessel, W. W.; Young, V. G., Jr.; Stein, A. *Dalton Trans.* **2003**, 4678–4681. (e) Liu, B.; Ku, Y.; Wang, M.; Zheng, P. *Inorg. Chem.* **1988**, *27*, 3868–3871.

(12) (a) Matsumoto, K. Y. *Bull. Chem. Soc. Jpn.* **1978**, *51*, 492–498. (b) Liu, B.-Y.; Xie, G.-Y.; Ku, Y.-T.; Wang, X. *Polyhedron* **1990**, *9*, 2023–2028. (c) Khan, M. I.; Zubieta, J. *Angew. Chem., Int. Ed.* **1994**, *33*, 760–762. (d) Khan, M. I.; Chang, Y.; Chen, Q.; Hope, H.; Parking, S.; Goshorn, D. P.; Zubieta, J. *Angew. Chem., Int. Ed.* **1992**, *31*, 1197–1200. (e) Johnson, B. J. S.; Schroden, R. C.; Zhu, C.; Young, V. G., Jr.; Stein, A. *Inorg. Chem.* **2002**, *41*, 2213–2218.

(13) (a) Kwak, W.; Rajkovic, L. M.; Stalick, J. K.; Pope, M. T.; Quicksall, C. O. *Inorg. Chem.* **1976**, *15*, 2778–2783. (b) Chang, Y.-D.; Zubieta, J. *Inorg. Chim. Acta* **1996**, *245*, 177–198. (c) Johnson, B. J. S.; Schroden, R. C.; Zhu, C.; Stein, A. *Inorg. Chem.* **2001**, *40*, 5972–5978. (d) Liu, B.-Y.; Ku, Y.-T.; Wang, X. *Inorg. Chim. Acta* **1989**, *161*, 233–237.

(14) (a) Salta, J.; Chang, Y.-D.; Zubieta, J. *J. Chem. Soc., Chem. Commun.* **1994**, 1039–1040. (b) Huan, G.; Johnson, J. W.; Jacobson, A. J.; Merola, J. S. *Chem. Mater.* **1990**, *2*, 719–723.

(15) Mason, M. R.; Mattews, R. M.; Mashuta, M. S.; Richardson, J. F.; Vij, A. *Inorg. Chem.* **1997**, *36*, 6476–6478.

(16) Xie, Y.-P.; Yang, J.; Ma, J.-F.; Zhang, L.-P.; Song, S.-Y.; Su, Z.-M. *Chem.—Eur. J.* **2008**, *14*, 4093–4103.

(17) (a) Yi, F.-Y.; Song, J.-L.; Zhao, N.; Mao, J.-G. *J. Solid State Chem.* **2008**, *181*, 1393–1401. (b) Yi, F.-Y.; Zhao, N.; Wu, W.; Mao, J.-G. *Inorg. Chem.* **2009**, *48*, 628–637.

(18) (a) Gao, E. Q.; Bai, S. Q.; He, Z.; Yan, C. H. *Inorg. Chem.* **2005**, *44*, 677–682. (b) Oshio, H.; Nihei, M.; Koizumi, S.; Shiga, T.; Nojiri, H.; Nakano, M.; Shirakawa, N.; Akatsu, M. *J. Am. Chem. Soc.* **2005**, *127*, 4568–4569. (c) Tasiopoulos, A. J.; Wernsdorfer, W.; Abboud, K. A.; Christou, G. *Angew. Chem., Int. Ed.* **2004**, *43*, 6338–6342. (d) Rajaraman, G.; Musugesu, M.; Sanudo, E. C.; Soler, M.; Wernsdorfer, W.; Helliwell, M.; Muryn, C.; Raftery, J.; Teat, S. J.; Christou, G.; Brechin, E. K. *J. Am. Chem. Soc.* **2004**, *126*, 15445–15457. (e) Price, D. J.; Batten, S. R.; Moubaraki, B.; Murray, K. S. *Chem. Commun.* **2002**, 762–763. (f) Wang, S.; Wemple, M. S.; Tsai, H. L.; Folting, K.; Huffman, J. C.; Hagen, K. S.; Hendrickson, D. N.; Christou, G. *Inorg. Chem.* **2000**, *39*, 1501–1513.

(19) (a) Ferreira, K. N.; Iverson, T. M.; Maghlaoui, K.; Barber, J.; Iwata, S. *Science* **2004**, *303*, 1831–1838. (b) Rutherford, A. W.; Boussac, A. *Science* **2004**, *303*, 1782–1784. (c) Mukhopadhyay, S.; Mandal, S. K.; Bhaduri, S.; Armstrong, W. H. *Chem. Rev.* **2004**, *104*, 3981–4026. (d) Dismukes, G. C. *Chem. Rev.* **1996**, *96*, 2909–2926.

(20) (a) Du, Z.-Y.; Li, X.-L.; Liu, Q.-Y.; Mao, J.-G. *Cryst. Growth Des.* **2007**, *7*, 1501–1507. (b) Du, Z.-Y.; Xu, H.-B.; Li, X.-L.; Mao, J.-G. *Eur. J. Inorg. Chem.* **2007**, 4520–4529. (c) Du, Z.-Y.; Prosvirin, A. V.; Mao, J.-G. *Inorg. Chem.* **2007**, *46*, 9884–9894.

Scheme 2. Free Ligand H_3L (a) and Its Coordination Modes in Compounds **1** (b, c), **2** and **4** (d), **3** (e), **5** (f, g), **6**, **7**, **9**, and **11** (f), **8** (d, f), **10** (h, i)

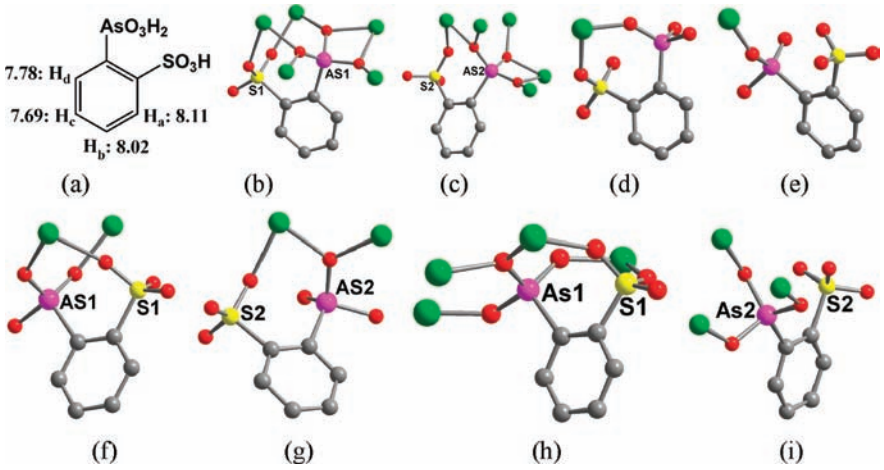

sulfonate-arsonate ligands. **10** contains an interesting heptanuclear cluster in which the Mn^{2+} centers are bridged by arsonate, sulfonate groups, and hydroxyl anions and **11** features a 1D chain in which each pair of Mn^{2+} centers are bridged by an arsonate group of a sulfonate-arsonate ligand. They represent the first structurally characterized metal sulfonate-arsonates. Herein, we report their syntheses, crystal structures, magnetic properties.

Experimental Section

Materials and Methods. The *o*-sulfophenylarsonic acid (*o*-$HO_3S-C_6H_4-AsO_3H_2$) was synthesized according to procedures described previously.[21] All of the other chemicals were obtained from commercial sources and used without further purification. Elemental analyses were performed on a German Elementary Vario EL III instrument. The FT-IR spectra were recorded on a Nicolet Magna 750 FT-IR spectrometer using KBr pellets in the range of 4000−400 cm^{-1}. Thermogravimetric analyses were carried out on a NETZSCH STA 449C unit at a heating rate of 10 °C/min under a static air atmosphere. X-ray powder diffraction (XRD) patterns (Cu−Kα) were collected on a PANalytical X'Pert PRO diffractometer. The ^1H NMR spectrum of the sulfonate-arsonate ligand was recorded on a Bruker Avance 400 spectrometer. The electrospray ionization mass spectrometry (ESI-MS) spectrum of the sulfonate-arsonate ligand was recorded on a ThermoFinnigan DECAX-30000 LCQ Deca XP ion trap mass spectrometer. Magnetic susceptibility measurements were carried out on a Quantum Design MPMSXL SQUID magnetometer and PPMS-9T system. The raw data were corrected for the susceptibility of the container and the diamagnetic contributions of the sample using Pascal constants.[22a]

Synthesis of the *o*-Sulfophenylarsonic Acid (H_3L). *o*-Sulfophenylarsonic acid (*o*-$HO_3S-C_6H_4-AsO_3H_2$) was synthesized according to the procedures previously described by Montoneri et al.[21] Phenylarsonic acid (12.12 g, 60 mmol) was added to freshly distilled SO_3 (11.52 g, 144 mmol) at 0 °C, and then the mixture was heated at 85−90 °C for 24 h. The phenylarsonic acid was converted to the *o*-sulfophenylarsonic acid. Residual SO_3 was converted to $BaSO_4$ by the addition of aqueous HCl and $BaCl_2$ to the reaction mixture in water. The excess Ba^{2+} ions were removed by passing a column filled with Dowex 50W-X8 H^+ form resin. The eluate was finally concentrated and dried, and the final product (H_3L) was obtained in a yield of about 65% based on phenylarsonic acid. ^1H NMR (400 MHz, D_2O): δ_{ppm} 8.11 (m, $1H_a$), 8.02 (m, $1H_b$), 7.78(m, $1H_d$), 7.69(m, $1H_c$) (Scheme 2a). IR (KBr, cm^{-1}): 3208 (s), 3096 (w), 1571 (w), 1461 (w), 1432 (m), 1254 (s), 1196 (s), 1156 (m), 1118 (m), 1059 (m), 1007 (s), 808 (m), 770 (vs), 747 (m), 710 (w), 663 (m), 619 (s), 560 (m), 483 (m). Negative ESI/MS *m*/*e* [ions] 281 for [*o*-$O_3S-C_6H_4-AsO_3H_2]^-$. Anal. Calcd (%) for H_3L: C, 25.55; H, 2.50; S, 11.37%. Found: C, 25.46; H, 2.50; S, 11.33%.

Synthesis of $Mn_3(L)_2(H_2O)_3\cdot(H_2O)$ (1). A mixture of $Mn(CH_3COO)_2\cdot 4H_2O$ (0.098 g, 0.4 mmol) and H_3L (0.056 g, 0.2 mmol) in 10 mL of deionized water was put into a Parr Teflon-lined autoclave (23 mL) and heated at 150 °C for 4 days. The initial pH value of the solution was 4.0. Pink-plate crystals of **1** were collected about 25% based on H_3L. Its purity was confirmed by XRD (see Supporting Information). Anal. Calcd (%) for $C_{12}H_{16}As_2Mn_3O_{16}S_2$ (M_r = 795.03): C, 18.13; H, 2.03. Found: C, 18.10; H, 2.03. IR data (KBr, cm^{-1}) for **1**: 3460 (m), 3091 (w), 2948 (w), 1615 (m), 1458 (w), 1426 (w), 1243 (s), 1172 (vs), 1145 (m), 1116 (m), 1064 (m), 1019 (vs), 964 (w), 878 (m), 848 (w), 817 (vs), 788 (m), 770 (w), 747 (w), 657 (m), 618 (m), 573 (w), 467 (w).

Syntheses of $[Mn(HL)(phen)_2]_2\cdot 8.5H_2O$ (2), $Mn(HL)(phen)_2(H_2O)\cdot 2H_2O$ (3), and $Mn_7(OH)_2(L)_4(phen)_8\cdot 10H_2O\cdot$phen (10). A mixture of $Mn(CH_3COO)_2\cdot 4H_2O$ (0.049 g, 0.2 mmol), H_3L (0.056 g, 0.2 mmol), and phen (0.079 g, 0.4 mmol) in 10 mL of deionized water was put into a Parr Teflon-lined autoclave (23 mL) and heated at 150 °C for 4 days. The initial pH values of the solutions are adjusted to 6.7 by the addition of 1 M NaOH solution. Very few crystals of **10** were collected. The resultant solution was allowed to evaporate slowly at room temperature; orange-brick-crystals of **2** and yellow-prism-crystals of **3** were collected in a yield of about 36% for **2**, and 51% for **3** based on H_3L. The purities of **2**−**3** were also confirmed by powder XRD (see Supporting Information). Many attempts were made to obtain a pure phase of compound **10** by changing the reaction conditions, such as Mn/L/phen molar ratios, pH values, and reaction temperatures, but were unsuccessful; the main purities are compounds **2**, **3**, and **5**. Because not enough samples were available, magnetic property measurements for **10** were not performed. Anal. Calcd (%) for **2**: C, 46.67; H, 3.85; N, 7.26.

(21) (a) Du, Z.-Y.; Xu, H.-B.; Mao, J.-G. *Inorg. Chem.* **2006**, *45*, 6424–6430. (b) Montoneri, E. *Phosphorus, Sulfur Silicon, Relat. Elem.* **1991**, *55*, 201–204. (c) Montoneri, E.; Gallazzi, M. C.; Grassi, M. *Dalton Trans.* **1989**, 1819–1823.

(22) (a) Kahn, O. *Molecular Magnetism*; VCH Publishers, Inc.: New York. 1993. (b) Ma, Y.-S.; Song, Y.; Du, W.-X.; Li, Y.-Z.; Zheng, L.-M. *Dalton Trans.* **2006**, 3228–3235. (c) Cao, D.-K.; Xie, X.-J.; Li, Y.-Z.; Zheng, L.-M. *Dalton Trans.* **2008**, 5008–5015. (d) Zhao, J.-P.; Hu, B.-W.; Yang, Q.; Hu, T.-L.; Bu, X.-H. *Inorg. Chem.* **2009**, *48*, 7111–7116. (e) Masuda, Y.; Kuratsu, M.; Suzuki, S.; Kozaki, M.; Shiomi, D.; Sato, K.; Takui, T.; Hosokoshi, Y.; Lan, X.-Z.; Miyazaki, Y.; Inaba, A.; Okada, K. *J. Am. Chem. Soc.* **2009**, *131*, 4670–4673. (f) Zhang, X.-M.; Zhang, X.-H.; Wu, H.-S.; Tong, M.-L.; Ng, S. W. *Inorg. Chem.* **2008**, *47*, 7462–7464.

Found: C, 46.51; H, 3.81; N, 7.21. For **3**: C, 48.08; H, 3.63; N, 7.48. Found: C, 47.97; H, 3.61; N, 7.45. IR data (KBr, cm^{-1}) for **2**: 3445 (s), 3060 (w), 2866 (w), 1622 (m), 1589 (w), 1574 (w), 1516 (m), 1450 (w), 1425 (vs), 1342 (w), 1249 (s), 1222 (w), 1181 (s), 1140 (s), 1112 (m), 1063 (m), 1018 (s), 957 (w), 910 (m), 865 (s), 772 (w), 731 (s), 659 (w), 635 (w), 616 (m), 568 (w), 557 (w), 459 (w). IR data (KBr, cm^{-1}) for **3**: 3427 (vs), 3060 (w), 2927 (w), 1623 (m), 1592 (w), 1517 (m), 1495 (w), 1452 (w), 1426 (s), 1342 (w), 1257 (s), 1174 (m), 1141 (m), 1112 (m), 1101 (w), 1060 (m), 1012 (s), 901 (m), 883 (s), 863 (m), 855 (m), 767 (w), 730 (s), 661 (w), 637 (w), 615 (m), 568 (w), 555 (w), 499 (w). IR data (KBr, cm^{-1}) for **10**: 3392 (w), 2978 (w), 2875 (w), 1619 (m), 1516 (m), 1427 (m), 1241 (w), 1228 (w), 1172 (w), 1121 (m), 1062 (w), 1018 (m), 863 (w), 853 (m), 732 (m).

Syntheses of Compounds 4−9 and 11. Compounds **4**−**9** and **11** were synthesized by a procedure similar to that used for **2** by altering the metal materials, the second auxiliary chelating ligand phen (or bipy, terpy), reaction temperature, and the molar ratio of starting materials. A mixture of $Mn(CH_3COO)_2 \cdot 4H_2O$ (0.049 g, 0.2 mmol), H_3L (0.056 g, 0.2 mmol), and phen (0.040 g, 0.2 mmol) in 10 mL of deionized water was put into a Parr Teflon-lined autoclave (23 mL) and heated at 150 °C for 4 days. The initial pH value of the solution is 3.5. Yellow-plate crystals of **5** were collected in a yield of about 72% based on H_3L. When bipy and terpy are used instead of phen under different molar ratio (Mn/H_3L/auxiliary ligand = 1:1:2 for **8**, 1:1:1 for **9** and **11**), yellow-brick crystals of **8** and **11** and salmon pink-brick crystals of **9** were collected in a yield of about 83% for **8**, 46% for **11**, and 86% for **9** based on H_3L.

When $Mn(ClO_4)_2 \cdot 6H_2O$ was used instead of $Mn(CH_3COO)_2 \cdot 4H_2O$, and the mixture was heated at 140 °C (for **4** and **6**) or 170 °C (**7**) for 4 days, yellow-brick crystals of **4**, **6**, and **7** were collected in a yield of about 74% for **4**, 75% for **6**, and 51% for **7** based on Mn, respectively.

The purities of these compounds were also confirmed by powder XRD (see Supporting Information). Anal. Calcd (%) for **4**: C, 43.09; H, 3.41; N, 7.73. Found: C, 43.21, H, 3.37; N, 7.70. For **5**: C, 41.24; H, 2.69; N, 5.34. Found: C, 41.19; H, 2.69; N, 5.31. For **6**: C, 46.33; H, 3.38; N, 8.01. Found: C, 46.28; H, 3.35; N, 8.00. For **7**: C, 48.20; H, 3.07; N, 8.33. Found: C, 48.12; H, 3.02; N, 8.30. For **8**: C, 42.95; H, 3.26; N, 7.15. Found: C, 42.89; H, 3.24, N, 7.11. For **9**: C, 44.38; H, 2.84; N, 7.39. Found: C, 44.31; H, 2.83; N, 7.35. For **11**: C, 35.38; H, 3.15; N, 5.16. Found: C, 35.28; H, 3.15; N, 5.10. IR data (KBr, cm^{-1}) for **4**: 3501 (w), 3076 (w), 2888 (w), 1597 (s), 1575 (w), 1566 (w), 1490 (w), 1474 (m), 1439 (vs), 1316 (m), 1254 (s), 1182 (m), 1169 (m), 1156 (m), 1144 (m), 1112 (s), 1060 (m), 1013 (vs), 968 (w), 910 (s), 764 (vs), 738 (s), 659 (m), 648 (w), 615 (s), 574 (m), 557 (w), 497 (w). IR data (KBr, cm^{-1}) for **5**: 3060 (w), 2324 (w), 1624 (w), 1592 (w), 1579 (w), 1519 (m), 1428 (s), 1349 (w), 1254 (s), 1174 (s), 1152 (w), 1117(m), 1065 (m), 1018 (s), 887 (m), 859 (m), 847 (m), 818 (m), 766 (m), 744 (m), 730 (m), 660 (m), 637 (w), 612 (m), 561 (m), 496 (w). IR data (KBr, cm^{-1}) for **6**: 3408 (m), 3073 (m), 1623 (m), 1590 (m), 1577 (w), 1516 (s), 1496 (w), 1452 (w), 1424 (vs), 1342 (m), 1299 (w), 1261 (m), 1223 (w), 1209 (w), 1182 (s), 1146 (s), 1104 (vs), 1019 (m), 930 (m), 863 (s), 850 (s), 765 (m), 745 (w), 730 (w), 724 (s), 660 (m), 637 (w), 616 (s), 577 (w), 562 (w), 496 (w). IR data (KBr, cm^{-1}) for **7**: 3427 (w), 3062 (w), 2363 (w), 1624 (m), 1591 (w), 1579 (w), 1518 (s), 1495 (w), 1452 (w), 1425 (s), 1343 (w), 1301 (w), 1255 (m), 1222 (w), 1176 (w), 1143 (m), 1103 (vs), 1018 (m), 895 (m), 865 (m), 848 (s), 773 (m), 744 (w), 730 (s), 660 (m), 638 (w), 623 (m), 577 (w). IR data (KBr, cm^{-1}) for **8**: 3426 (m), 3082 (w), 2921 (w), 2352 (w), 1632 (w), 1595 (m), 1575 (w), 1490 (w), 1474 (m), 1439 (s), 1311 (w), 1254 (s), 1186 (vs), 1142 (m), 1112 (m), 1061 (m), 1016 (vs), 964 (w), 919 (m), 870 (s), 767 (s), 739 (s), 718 (m), 659 (m), 614 (s), 576 (m), 558 (w), 503 (w). IR data (KBr, cm^{-1}) for **9**: 2416 (w), 1595 (m), 1572 (w), 1475 (w), 1451 (m), 1439 (w), 1428 (w), 1312 (w), 1295 (w), 1237 (s), 1197 (s), 1164 (w), 1136 (w), 1114 (w), 1060 (m), 1037 (w), 1016 (s), 977 (w), 953 (w), 922 (s), 885 (m), 850 (w), 831 (w), 809 (w), 772 (s), 739 (m), 721 (w), 706 (m), 682 (w), 664 (m), 637 (w), 619 (m), 598 (w). IR data (KBr, cm^{-1}) for **11**: 3501 (s), 3069 (w), 2803 (w), 2433 (w), 1658 (w), 1596 (m), 1574 (w), 1490 (w), 1475 (m), 1440 (m), 1316 (w), 1234 (s), 1197 (vs), 1153 (w), 1142 (m), 1116 (m), 1065 (m), 1019 (s), 966 (w), 892 (vs), 832 (m), 768 (s), 736 (s), 658 (m), 615 (m), 563 (m), 491 (m), 456 (w).

Caution! *Perchlorate salts are potentially explosive and should be used in small amounts and handled with care.*[23]

Single-Crystal Structure Determination. Data collections were performed on a Saturn 70 CCD diffractometer (for **1**, **2**, **5**, **8**−**11**) and a Rigaku Mercury CCD diffractometer (for **3**, **4**, **6**, **7**). All diffractometers were equipped with a graphite-monochromated Mo−Kα radiation (λ = 0.71073 Å). Intensity data for all eleven compounds were collected by the narrow frame method at 293(2) K. The data sets were corrected for Lorentz and Polarization factors as well as for absorption by a Multiscan method (for **1**−**11**).[24] All eleven structures were solved by the direct methods and refined by full-matrix least-squares fitting on F^2 by SHELX-97.[24] All non-hydrogen atoms were refined with anisotropic thermal parameters, except O(6W), O(7W), O(8W), and O(9W) in **2**, and O(14), O(22), O(23), O(24), and O(24′) in **6**, which were refined with isotropic thermal parameters. Several atoms of the free phen ligand (N(11), C(61), C(62), C(63)) in **10** are disordered and each atom displays two symmetry related sites; hence, the occupancy factors of these atoms are reduced by 50%. The oxygen atoms of the perchlorate anions (O(11) associated with $Cl(1)O_4$ and O(24) associated with $Cl(2)O_4$ in **6** and O(14) associated with $Cl(1)O_4$ in **7**) are also disordered and each exhibits two sites with 50% occupancy. The lattice water molecules (O(3W) and O(3W′)) in **3**, O(6W) and O(6W′) in **10**, O(3W) and O(3W′) in **11** are also disordered over two orientations; hence, the occupancy factor of each site was fixed to be 50%. The occupancy factors of O(9W) in **2**, O(5W) and O(6W) in **6**, O(3W), O(4W), O(5W), and O(7W) in **10** were reduced to 50% because of their large thermal parameters. All hydrogen atoms associated with C atoms, arsonate groups, and some water molecules were located at geometrically calculated positions and refined with isotropical thermal parameters. Crystallographic data and structural refinements for compounds **1**−**11** are summarized in Table 1. Important bond lengths are listed in Table S1, Supporting Information. More details on the crystallographic studies as well as atomic displacement parameters are given as Supporting Information.

Results and Discussion

Hydrothermal reactions of manganese(II) salts with *o*-sulfophenylarsonic acid (H_3L = *o*-$HO_3S-C_6H_4-AsO_3H_2$) afforded $Mn_3(L)_2(H_2O)_3 \cdot H_2O$ (**1**) with a layered structure. When various auxiliary chelating ligands such as phen, bipy, and terpy were used, various types of lower dimensional assemblies including mononuclear, dinuclear, and heptanuclear clusters as well as 1D chain were isolated. They represent the first structurally characterized metal sulfonate-arsonates. These results also provide valuable insights to the rational design of low dimensional materials. Several possible factors that affect the types of structures formed include the M/L and M/second ligand molar ratios, the number of available donor atoms of the second ligand, the coordination geometries

(23) Wolsey, W. C. *J. Chem. Educ.* **1973**, *50*, A335 and references therein.

(24) (a) Sheldrick, G. M. *Program SADABS*; Universität Göttingen: Göttingen, Germany, 1995. (b) *CrystalClear*, version 1.3.5; Rigaku Corp.: Woodlands, TX, 1999. (c) Sheldrick, G. M. *SHELX-96 Program for Crystal Structure Determination*; Siemens Analytical X-ray Instruments: Madison, WI, 1996.

Table 1. Summary of Crystal Data and Structure Refinements for **1**−**11**

	1	**2**	**3**	**4**	**5**	**6**
empirical formula	$C_{12}H_{16}As_2Mn_3O_{16}S_2$	$C_{60}H_{59}As_2Mn_2N_8O_{20.5}S_2$	$C_{30}H_{27}AsMnN_4O_9S$	$C_{52}H_{49}As_2ClMn_2N_8O_{19}S_2$	$C_{36}H_{28}As_2Mn_2N_4O_{13}S_2$	$C_{54}H_{47}AsCl_2Mn_2N_8O_{19}S$
formula weight	795.03	1543.99	749.48	1449.28	1048.46	1399.76
crystal system	monoclinic	triclinic	triclinic	triclinic	triclinic	triclinic
space group	$P2_1/c$	$P\bar{1}$	$P\bar{1}$	$P\bar{1}$	$P\bar{1}$	$P\bar{1}$
a (Å)	12.6794(13)	15.525(3)	10.5222(18)	8.9739(3)	7.967(2)	14.285(4)
b (Å)	13.2537(11)	16.197(3)	12.801(3)	15.70830(10)	11.658(3)	14.874(5)
c (Å)	13.7316(12)	16.287(3)	13.644(2)	21.7523(12)	21.204(6)	15.715(5)
α (deg)	90	68.629(11)	111.433(4)	75.713(11)	81.509(7)	68.834(12)
β (deg)	94.818(5)	65.072(10)	93.179(2)	83.861(14)	81.607(8)	72.813(13)
γ (deg)	90	62.493(10)	112.781(5)	74.266(13)	76.162(8)	73.420(13)
V (Å^3)	2299.4(4)	3219.8(10)	1535.1(5)	2857.50(19)	1878.6(9)	2914.4(15)
Z	4	2	2	2	2	2
D_{calcd} (g cm^{-3})	2.297	1.593	1.621	1.684	1.853	1.595
μ (mm^{-1})	4.737	1.559	1.629	1.794	2.606	1.206
GOF	1.085	1.069	0.950	1.060	1.034	1.050
R_1, wR_2 [$I > 2\sigma(I)$][a]	0.0473, 0.1007	0.0722, 0.1869	0.0601, 0.1320	0.0613, 0.1429	0.0340, 0.0765	0.0706, 0.1863
R_1, wR_2 [all data]	0.0589, 0.1068	0.1223, 0.2258	0.1049, 0.1573	0.0886, 0.1585	0.0486, 0.0829	0.0984, 0.2131

	7	**8**	**9**	**10**	**11**
empirical formula	$C_{54}H_{41}AsCl_2Mn_2N_8O_{16}S$	$C_{42}H_{38}As_2Mn_2N_6O_{14}S_2$	$C_{42}H_{32}As_2Mn_2N_6O_{12}S_2$	$C_{124}H_{110}As_4Mn_7N_{20}O_{36}S_4$	$C_{16}H_{17}AsMnN_2O_9S$
formula weight	1345.71	1174.62	1136.58	3268.82	543.24
crystal system	monoclinic	triclinic	triclinic	monoclinic	monoclinic
space group	$P2_1/n$	$P\bar{1}$	$P\bar{1}$	$P2_1/n$	$P2_1/c$
a (Å)	13.840(4)	11.061(4)	8.512(3)	20.48(3)	11.285(4)
b (Å)	28.893(7)	13.475(4)	10.030(4)	14.630(6)	7.971(3)
c (Å)	15.263(4)	16.785(5)	13.327(5)	24.14(2)	22.609(7)
α (deg)	90	91.401(2)	87.898(11)	90	90
β (deg)	113.175(4)	106.996(3)	71.709(9)	97.189(15)	93.014(5)
γ (deg)	90	106.981(4)	78.920(12)	90	90
V (Å^3)	5611(2)	2271.6(13)	1059.8(7)	7178(14)	2030.9(11)
Z	4	2	1	2	4
D_{calcd} (g cm^{-3})	1.593	1.717	1.781	1.512	1.777
μ (mm^{-1})	1.246	2.168	2.317	1.650	2.422
GOF	1.078	1.031	0.935	1.148	1.044
R_1, wR_2 [$I > 2\sigma(I)$][a]	0.0493, 0.1288	0.0577, 0.1071	0.0362, 0.0689	0.0939, 0.2408	0.0615, 0.1349
R_1, wR_2 [all data]	0.0621, 0.1385	0.1097, 0.1328	0.0652, 0.0774	0.1258, 0.2650	0.0977, 0.1555

[a] $R_1 = \sum||F_o| - |F_c||/\sum|F_o|$, $wR_2 = \{\sum w(F_o^2 - F_c^2)^2/\sum w(F_o^2)^2\}^{1/2}$.

around the metal ions, the aqua ligand, the counteranion as well as the coordination mode of the arsonate ligand. For example, using $Mn(CH_3COO)_2 \cdot 4H_2O$ as the metal source and phen as the auxiliary ligand, **5** was obtained whereas **6** and **7** were isolated when $Mn(ClO_4)_2 \cdot 6H_2O$ was used as metal source (the reacting temperature was increased to 170 °C for **7**). **2**, **3** and **10** were obtained by changing the pH value from 3.0 to 6.7 by the addition 1 M NaOH. Using bipy or terpy instead of phen affords **4**, **8**, **9**, and **11**. When second ligand/M molar ratio is 2, mononuclear complexes are most likely to form since only one or two coordination sites are left for the arsonate ligand as in **2**−**4**. When the second ligand/M molar ratio is between 2 and 1, more coordination sites are left, dinuclear clusters such as **5**−**9** or a 1D chain such as **11** was obtained. The *o*-sulfophenylarsonic acid is a versatile ligand and is able to adopt many types of coordination modes (8 modes are observed in **1**−**11**) (Scheme 2). The sulfonate-arsonate ligand is apt to form a seven chelating ring (Mn−O−As−C−C-S-O) in all eleven compounds isolated except **3**. Compared with *m*-sulfophenylphosphonate, the *o*-sulfophenylarsonate is apt to bind with fewer metal centers.[20c]

Structure of $Mn_3(L)_2(H_2O)_3 \cdot H_2O$ (1). There are three unique manganese(II) ions, two $\{L\}^{3-}$ anions, three aqua ligands, and one lattice water molecule in the asymmetric unit of **1** (Figure 1). Each Mn(II) ion is octahedrally coordinated by an aqua ligand, one sulfonate oxygen atom, and four arsonate oxygen atoms. The Mn−O distances are in the range of 2.094(2)−2.288(2) Å, which are compared to those reported in other manganese(II) phenylarsonates and manganese(II) phenylphosphonates.[17b,20,25a−f]

The two unique L^{3-} anions in **1** adopt two different types of coordination modes (Scheme 2). The ligand containing As(1) and S(1) is octadentate and bridges to five metal ions, all three arsonate oxygens are bidentate, two sulfonate oxygens are unidentate, and the third one remains non-coordinated (Scheme 2b). The ligand containing As(2) and S(2) is heptadentate and also bridges with five metal ions, the only difference is that only one sulfonate oxygen is bonded to the metal center (Scheme 2c).

Each pair of $Mn(1)O_6$ and $Mn(2)O_6$ octahedra forms a dimer via edge-sharing, these dimers are bridged by

(25) (a) Mao, J.-G.; Wang, Z.-K.; Clearfield, A. *Inorg. Chem.* **2002**, *41*, 2334–2340. (b) Yang, B.-P.; Mao, J.-G. *Inorg. Chem.* **2005**, *44*, 566–571. (c) Bao, S. S.; Chen, G.-S.; Wang, Y.; Li, Y.-Z.; Zheng, L.-M.; Luo, Q.- H. *Inorg. Chem.* **2006**, *45*, 1124–1129. (d) Yin, P.; Gao, S.; Wang, Z.-M.; Yan, C.-H.; Zheng, L.-M.; Xin, X.-Q. *Inorg. Chem.* **2005**, *44*, 2761–2765. (e) Merrill, C. A.; Cheetham, A. K. *Inorg. Chem.* **2007**, *46*, 278–284. (f) Ma, Y.-S.; Yao, H.-C.; Hua, W.-J.; Li, S.-H.; Li, Y.-Z.; Zheng, L.-M. *Inorg. Chim. Acta* **2007**, *360*, 1645–1650. (g) Thirumurugan, A.; Sanguramath, R. A.; Rao, C. N. R. *Inorg. Chem.* **2008**, *47*, 823–831.

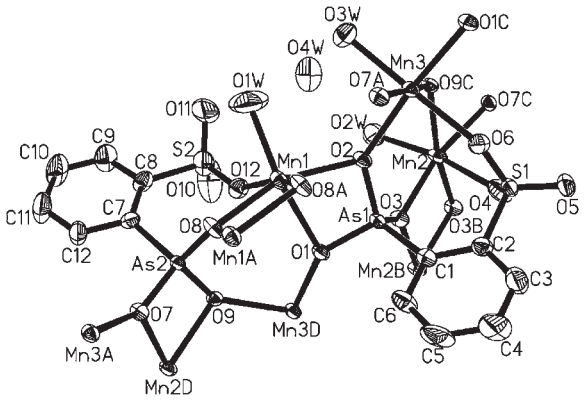

Figure 1. ORTEP representation of the selected unit in compound **1**. The thermal ellipsoids are drawn at 50% probability level. Symmetry code for the generated atoms: (a) $-x+1, -y+1, -z$. (b) $-x+1, -y+2, -z$. (c) $x, -y+3/2, z+1/2$. (d) $x, -y+3/2, z-1/2$.

$Mn(3)O_6$ octahedra via corner-sharing into a layered manganese(II) oxide sheet with Mn_5 five-member rings (Figure 2a).[25g] The Mn···Mn separations within a pair of edge-sharing octahedra are 3.270(1) and 3.282(1) Å, respectively for the Mn(1) and Mn(2) dimers. The Mn···Mn distances between two corner-sharing MnO_6 octahedra are much longer, being in the range of 3.992(1)−4.071(1) Å. The arsonate groups are capped on Mn_5 five-member rings whereas the sulfonate groups are hanging on the 2D sheet (Figure 2b). The organic groups of the sulfonate-arsonate ligands are orientated toward the interlayer space (Figure 2b). The lattice water molecules are also located at the interlayer space. The 2D layers are held together via the weak van der Waals force (Supporting Information, Figure S3).

Structures of $[Mn(HL)(phen)_2]_2 \cdot 8.5H_2O$ (2), $Mn(HL)(phen)_2(H_2O) \cdot 2H_2O$ (3), and $[Mn(HL)(bipy)_2][Mn(H_2L)(bipy)_2](ClO_4) \cdot 3H_2O$ (4). They all contain mononuclear metal arsonate units, namely, $[Mn(HL)(phen)_2]$ for **2** and **3**, and $[Mn(HL)(bipy)_2]$ and $[Mn(H_2L)(bipy)_2]^+$ for **4** (Figure 3). The main difference lies in the number of the mononuclear unit, aqua ligands, counteranion, and guest water molecules. There are two mononuclear units, and eight and a half lattice water molecules in **2**; one mononuclear, an aqua ligand, and two lattice water molecules in **3**; two mononuclear units, one perchlorate anion and three lattice water molecules in **4**. In compounds **2** and **4**, the Mn(II) ion is octahedrally coordinated by one arsonate oxygen, one sulfonate oxygen from one sulfonate-arsonate anion, and four nitrogen atoms from two phen ligands (or bipy ligands). The Mn(II) ion in compound **3** is also octahedrally coordinated, the only difference is that the coordination sulfonate oxygen atom is replaced by an aqua ligand. The sulfophenylarsonate ligands in compounds **2** and **3** are singly protonated, whereas in compound **4** one sulfophenylarsonic acid ligand is singly protonated and the other one is doubly protonated as indicated by the elongated As−O bonds (Supporting Information, Table S1). In **2** and **4**, the arsonate-sulfonate ligand is bidentately chelating with a Mn(II) ion by using one sulfonate and one arsonate oxygen atoms, the other O-donors remain non-coordinated (Scheme 2d). The HL^{2-} dianion in **3** is monodentate and bonded to one Mn(II) ion by using one arsonate oxygen atom,

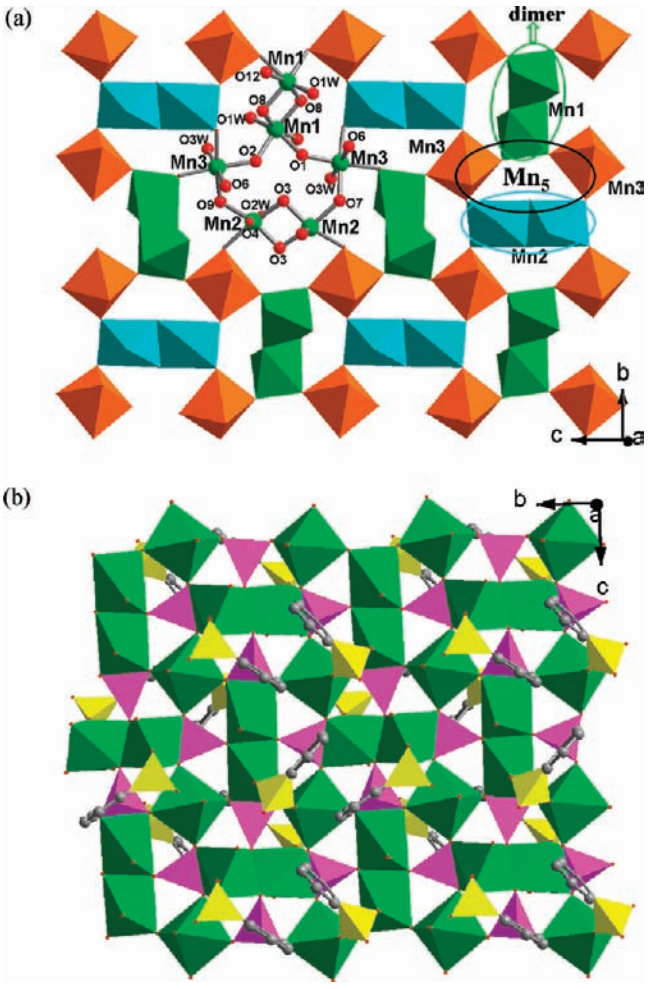

Figure 2. (a) Mn−O layer in **1**. $Mn(1)O_6$, $Mn(2)O_6$, and $Mn(3)O_6$ octahedra are shaded in green, cyan, and orange, respectively. (b) View the 2D layer of compound **1** along *a*-axis. The CSO_3 and $CAsO_3$ tetrahedra are shaded in yellow and purple, respectively. MnO_6 octahedra are shaded in green. C atoms are represented by middle gray circles.

the other oxygen atoms remain non-coordinated (Scheme 2e).

In **2**, a pair of mononuclear cluster units containg Mn(1) are linked into a dinuclear cluster unit via hydrogen bonds between singly protonated arsonate oxygen atom (O(1)) and non-coordination arsonate atom (O(3)). The O···O separation is 2.618(6) Å (symmetry code: $-x, -y+1, -z+1$) (Supporting Information, Figure S1). A pair of mononuclear cluster units containing Mn(2) are also linked into a dinuclear cluster unit via hydrogen bonds among water molecules (O(2W), O(4W)), non-coordination arsonate atom (O(7) and O(12)). The O···O separations are in the range of 2.67(2)−2.78(1) Å (Supporting Information, Figure S1). The dinuclear cluster units are assembled into a 3D supramolecular structure via weak $\pi \cdots \pi$ interactions between aromatic ring of the phen ligands (Supporting Information, Table S3, Figure S3). The distances between centers of these aromatic rings are in the range of 3.544−3.967 Å, and the corresponding dihedral angles fall in the range of 0−2.2°.

In **3**, the discrete mononuclear cluster units are linked into a 1D chain structure via hydrogen bonds among singly protonated oxygen atom (O(4)) and non-coordination

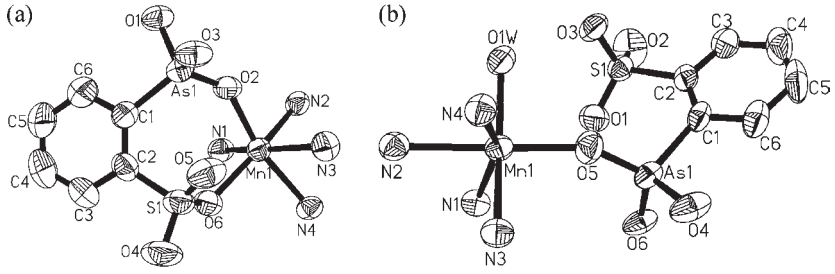

Figure 3. ORTEP representation of the mononuclear unit in compounds **2** and **4** (a) as well as **3** (b). The thermal ellipsoids are drawn at 50% probability level. The carbon atoms from phen (or bipy), all lattice water molecules, and the perchlorate anion have been omitted for clarity.

arsonate oxygen atom (O(6)), aqua ligand (O(1W)) and non-coordination sulfonate oxygen atom (O(3)). The O···O separations are in the range of 2.576(5)−2.752(5) Å (Supporting Information, Figure S2a). In **4**, the discrete mononuclear cluster units are also linked into a 1D chain structure via hydrogen bonds among singly protonated oxygen atoms (O(3), O(7)), non-coordination sulfonate oxygen atom (O(6)), and aqua ligands (O(2W), O(3W)). The O···O separations are in the range of 2.614(6)−2.952(6) Å (Supporting Information, Figure S2b). The 1D chains are further assembled into a 3D supramolecular structure via weak $\pi\cdots\pi$ interactions between aromatic ring of the phen and bipy ligands Supporting Information, (Table S3, Figure S3).

The shortest intermolecular Mn···Mn separations are 8.772(1), 7.814(1), and 7.805(1) Å respectively for compounds **2**−**4**.

Structures of [Mn(HL)(phen)][Mn(HL)(phen)(H$_2$O)] (5) and [Mn(HL)(terpy)]$_2$ (9). Both compounds display dinuclear cluster units based on a pair of O−As−O linkages whereas compound **5** contains an additional dinuclear cluster based on Mn_2O_2 ring (Figures 4a and 4c). In **5**, Mn(1) is five-coordinated by the two arsonate oxygen atoms and one sulfonate oxygen atom from two $\{HL\}^{2-}$ anions, and a bidentate-chelating phen ligand with a square pyramidal geometry, and the six-coordinated Mn(2) is bonded to an additional aqua ligand. The structure of the dinuclear cluster in **9** can be viewed as the bidentate phen ligand of the [Mn(HL)(phen)] unit in **5** being replaced by tridentate terpy; hence, the Mn^{2+} ion becomes octahedrally coordinated. The Mn−O and Mn−N distances fall in the range of 2.064(2)−2.341(2) Å and 2.284(2)−2.311(3) Å for compound **5**, and 2.078(2)−2.314(2) Å and 2.237(2)−2.304(3) Å for compound **9**.

There are two unique $\{HL\}^{2-}$ dianions in **5**. Although both of them are tridentate and bridging with two metal ions, they adopt two different coordinated modes (Scheme 2f and 2g). In both cases, the ligand forms a Mn−O−As−C−C−S−O seven member chelating ring and also bridges with the second metal ion. The main difference arises from the arsonate oxygen atom bridging to the second metal. In Scheme 2f, two arsonate oxygen atoms are involved in metal coordination whereas in the Scheme 2g mode only one arsonate oxygen atom is involved.

A pair of Mn(II) ions in **5** are bridged by a pair of arsonate groups into two different dinuclear cluster units: $[Mn_2(HL)_2(phen)_2]$ with a $Mn_2As_2O_4$ eight-member ring (Mn···M_n 4.0611(9) Å) and $[Mn_2(HL)_2(phen)_2(H_2O)_2]$ with a Mn_2O_2 four-member ring (Mn···M_n 3.4659(8) Å). The Mn−O−Mn angle in the $[Mn_2(HL)_2(phen)_2(H_2O)_2]$ cluster is 106.22(2)°. The $\{HL\}^{2-}$ dianion in **9** adopts a same coordination mode as that for $[Mn_2(HL)_2(phen)_2]$ in **5** (Scheme 2e). The Mn···Mn separation within the $[Mn_2(HL)_2(terpy)_2]$ dinuclear cluster unit is 5.205(2) Å, being much larger than those of $[Mn_2(HL)_2(phen)_2]$ in **5**.

These discrete dinuclear clusters in **5** are linked into a 1D double chain structure via hydrogen bonds (Supporting Information, Table S1, Figure 4b). A number of hydrogen bonds are formed among aqua ligands and non-coordination phenylarsonate oxygen atoms with O···O separations in the range of 2.570(3)−2.719(3) Å. These 1D chains are further assembled into a 2D layer by the $\pi\cdots\pi$ interactions between neighboring aromatic rings of the phen ligand and $\{HL\}^{2-}$ anion (Supporting Information, Table S3). These 2D layers are held together by the weak van der Waals force (Supporting Information, Figure S3). The dinuclear cluster units of compound **9** are also held together by the weak van der Waals force (Supporting Information, Figure S3). The shortest intercluster Mn···Mn distances is 7.729(1) Å for **5** or 8.512(1) Å for **9**.

Structures of [Mn$_2$(HL)(phen)$_4$(H$_2$O)](ClO$_4$)$_2$·4H$_2$O (6), [Mn$_2$(HL)(phen)$_4$(H$_2$O)](ClO$_4$)$_2$·H$_2$O (7), and Mn$_2$(HL)$_2$(bipy)$_3$(H$_2$O)·H$_2$O (8). All three compounds feature dinuclear cluster units in which the two manganese(II) centers are interconnected by only one bridging arsonate group, which are different from those in **5** and **9** discussed earlier (Figure 5). The only difference between compounds **6** and **7** is the number of lattice water molecules. The cluster unit in **8** can be considered as the four phen ligands in **6** and **7** being replaced by one bidentate chelating $\{HL\}^{2-}$ dianion and three bipy ligands.

There are two unique manganese(II) ions in **6**−**8**. One of them is octahedrallly coordinated by a $\{HL\}^{2-}$ dianion in a bidentate chelating fashion as well as four nitrogen atoms from two phen or bipy ligands. The second metal ion in **6**−**7** is octahedrally coordinated by four nitrogen atoms from two phen ligands, one arsonate oxygen atom from a $\{HL\}^{2-}$ dianion, and an aqua ligand, whereas in **8** it is six-coordinated by one bidentate chelating bipy ligand, one bidentate chelating $\{HL\}^{2-}$ dianion, one arsonate oxygen from another $\{HL\}^{2-}$ dianion, and an aqua ligand. The Mn−O and Mn−N distances are in the normal ranges and are comparable to those in **1**−**5** (Supporting Information, Table S1). The Mn···Mn separations between the two metal centers in the cluster units are 6.624(1) Å, 5.547(2) Å, and 5.830(2) Å

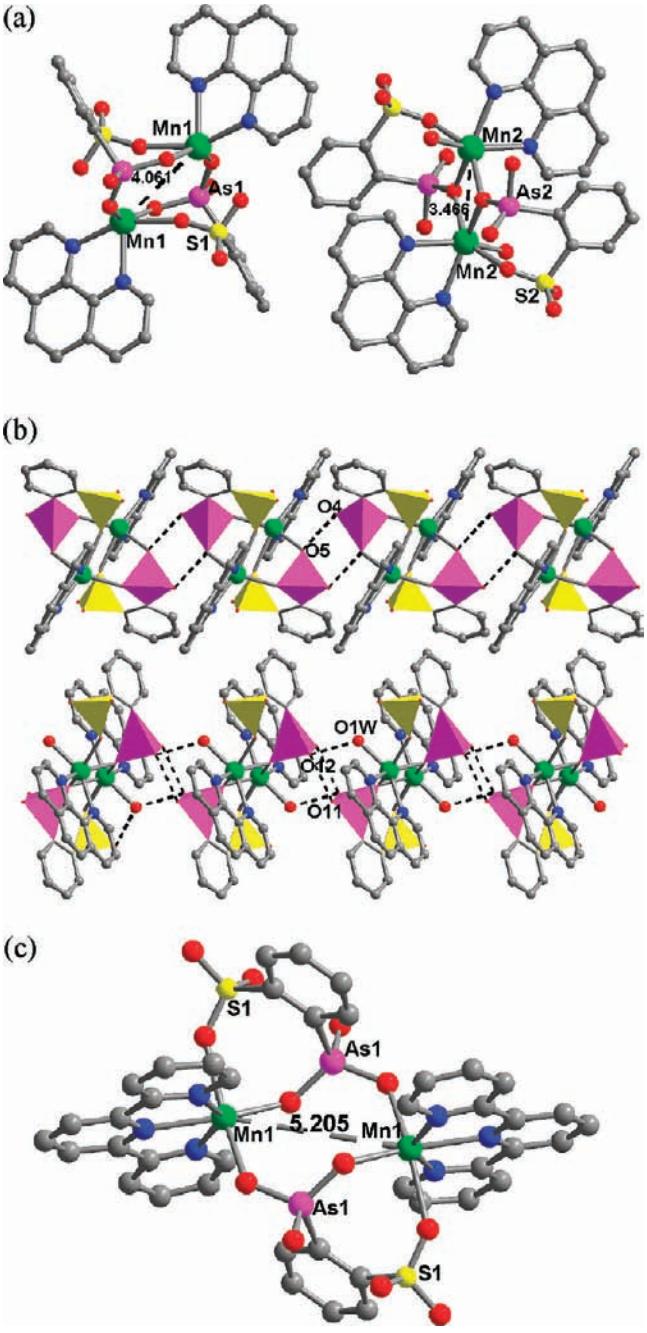

Figure 4. (a) Two different dinuclear cluster units in compound **5** with labeling of some Mn···Mn distances. (b) View of the 1D chain of the compound **5**. Hydrogen bonds are drawn as dashed lines. Mn, As, S, O, N, and C atoms are drawn as bright green, purple, yellow, red, blue, and medium gray circles, respectively. (c) The dinuclear cluster unit in compound **9**.

respectively for **6**, **7**, and **8**. The intercluster Mn···Mn distances are much larger, being at least 9.034(1), 8.226(2), and 7.722(2) Å respectively for **6**, **7** and **8**.

The arsonate-sulfonate ligands in **6** and **7** are tridentate, forming a bidentate chelation with a metal center and also bridges with a second metal center (Scheme 2f). In **8**, there is an additional arsonate-sulfonate ligand which only forms a bidentate chelation with a metal center (Scheme 2d).

The dinuclear clusters in **6** are linked into a 3D supramolecular structure via hydrogen bonds as well as the

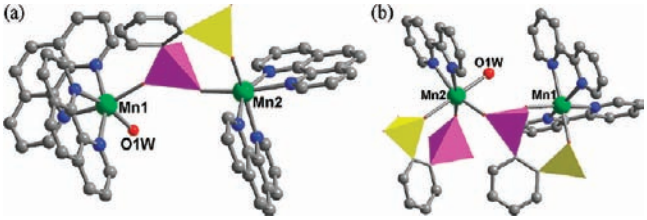

Figure 5. Dinuclear cluster units in **6** and **7** (a) and **8** (b). The arsonate and sulfonate groups are shaded in purple and yellow, respectively.

$\pi\cdots\pi$ packing interactions among aromatic rings of the phen ligands and $\{HL\}^{2-}$ anions (Supporting Information, Table S3, Figure S3). A number of hydrogen bonds are formed among water molecules, aqua ligand, perchlorate anion oxygen atoms, and non-coordination arsonate oxygen atoms. The O···O separations are in the range of 2.44(2)−2.885(7) Å (Supporting Information, Table S2). The dinuclear clusters in compound **7** are assembled into a 3D supra-molecular network by only weak $\pi\cdots\pi$ packing interactions between phen ligands (Supporting Information, Figure S3, Table S3). The dinuclear clusters in **8** are cross-linked into a 1D chain via hydrogen bonds among singly protonated oxygen atom (O(8)) and non-coordination arsonate oxygen atom (O(9)), lattice water molecule (O(2W)), aqua ligand (O(1W)), non-coordination arsonate oxygen atom (O(7)), and sulfonate oxygen atom (O(4)) (Supporting Information, Figure S2c). The O···O separations range from 2.557(5) to 2.886(6) Å (Supporting Information, Table S2). These 1D chains are further assembled into a 2D sheet via weak $\pi\cdots\pi$ packing interactions (Supporting Information, Table S3), and the latter are held together by the weak van der Waals force (Supporting Information, Figure S3).

Structure of $Mn_7(OH)_2(L)_4(phen)_8\cdot 10H_2O\cdot phen$ (10). Compound **10** features a novel heptanuclear cluster (Figure 6) with additional lattice waters and a free phen ligand as guest molecules. There are four unique metal ions and two unique L^{3-} anions in the asymmetric unit of **10**. Mn(1) is octahedrally coordinated by two arsonate oxygen atoms and one sulfonate oxygen atom from two $\{L\}^{3-}$ ligands, one hydroxyl anion and a bidentate-chelating phen ligand. Mn(2) is five-coordinated by two arsonate oxygen atoms from two $\{L\}^{3-}$ ligands, one hydroxyl anion, and a bidentate-chelating phen ligand. Mn(3) located at an inversion center is octahedrally coordinated by four arsonate oxygen atoms in a square plane from four $\{L\}^{3-}$ ligands and two hydroxyl anions in the axial positions. Mn(4) is in an octahedral geometry composed of one arsonate oxygen atom and one sulfonate oxygen atom from one $\{L\}^{3-}$ ligand and two bidentate-chelating phen ligands in *cis*-fashion. The Mn−O and Mn−N distances are in the range of 1.869(4)−2.320(5) Å and 2.106(6)−2.316(7) Å, respectively, which are comparable to those in **1**−**9**. The two unique sulfophenylarsonate anions adopt two unique coordination modes which are different from those in **1**−**9**. The L^{3-} anion containing As(1) and S(1) is hexadentate and bridges with four Mn(II) ions, two arsonate oxygen atoms are unidentate whereas the third one is bidentate, and two sulfonate oxygen atoms are also unidentate but the third one remains non-coordinated (Scheme 2h).

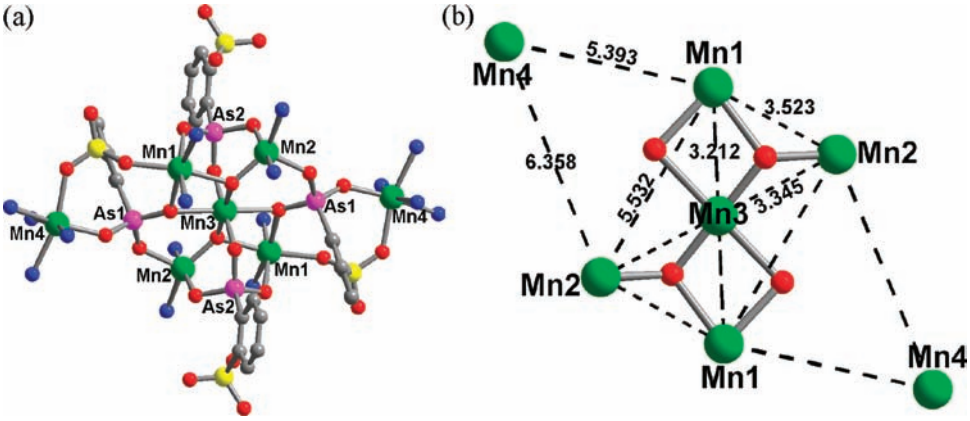

Figure 6. Heptanuclear cluster units in compound **10** (a) and the Mn···Mn distances within the cluster (b). Mn, As, S, O, N, and C atoms are drawn as bright green, purple, yellow, red, blue, and medium gray circles, respectively.

The L^{3-} anion ligand containing As(2) and S(2) is tridentate and bridges with three Mn(II) ions by using three arsonate oxygen atoms in a unidentate fashion, and the sulfonate group remains non-coordinated (Scheme 2i). The hydroxyl anion is tridentate and located at the center of a Mn_3 triangle.

Mn(II) ions are interconnected into a heptanuclear cluster by bridging L^{3-} and hydroxyl anions with the organic groups orientated toward the out-sphere of the cluster (Figure 6). The center $Mn(3)O_6$ octahedra shares two edges with two $Mn(1)O_4N_2$ octahedra, and two corners with two $Mn(2)O_3N_2$ square pyramids, forming a rectangular-shaped Mn_5 unit which is further attached by two $Mn(4)O_2N_4$ octahedra in the *trans* fashion via two Mn(2)−O−As(1)−O−Mn(4) and two Mn(1)−O−S(1)−O−Mn(4) bridges, resulted in the formation of a novel heptanuclear cluster unit. Such a type of heptanuclear clusters has not been reported. The Mn···Mn separations between edge-sharing polyhedra are 3.212(1) Å, and those between corner-sharing ones are 3.523(1) Å whereas those interconnected via Mn−O−As−O−Mn or/and Mn−O−S−O−Mn bridges are in the range of 5.393(1)−6.353(1) Å. These heptanuclear clusters are separated by guest molecules (free phen and lattice water molecules) and are assembled into a 3D supra-molecular assembly by weak hydrogen bonding among non-coordinated sulfonate oxygens and lattice water molecules and $\pi\cdots\pi$ interactions (Supporting Information, Table S3, Figure S3).

Structure of Mn(HL)(bipy)(H_2O)·$2H_2O$ (11). There is one unique manganese(II) ion, one $\{HL\}^{2-}$ ion, one bipy ligand, one aqua ligand as well as two lattice water molecules in the asymmetric unit of **11**. The Mn(II) is octahedrally coordinated by one bidentate chelating bipy ligand, one sulfonate oxygen atom and two arsonate oxygen atoms from two $\{HL\}^{2-}$ anions. The Mn−O and Mn−N distances fall in the ranges of 2.099(4)−2.247(4) Å and 2.234(4)−2.265(5) Å, respectively, which are comparable to those in **1**−**10**. The $\{HL\}^{2-}$ anion is tridentate and bridges with two metal ions, which is similar to those in compounds **6**, **7**, and **9** (Scheme 2f). The interconnection of neighboring Mn(II) ions by the bridging and chelating $\{HL\}^{2-}$ anions resulted into a 1D chain along *b*-axis (Figure 7a). Neighboring 1D chains are further interlinked into a (−201) supra-molecular

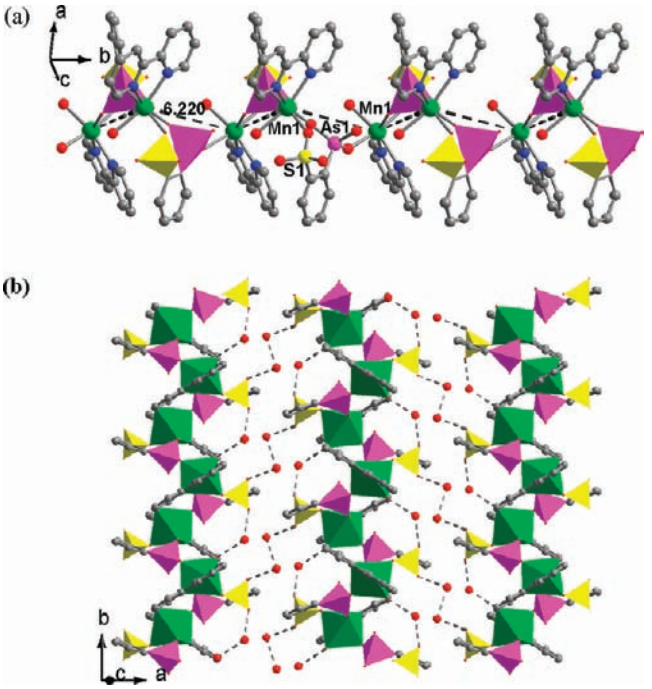

Figure 7. View of a 1D chain (a) and hydrogen bonded 2D layer in **11**. Mn, As, S, O, N, and C atoms are drawn as bright green, purple, yellow, red, blue, and medium gray circles, respectively.

layer via hydrogen bonds among aqua ligands, lattice water molecules, and non-coordination sulfonate oxygen atoms of the $\{HL\}^{2-}$ anions (Figure 7b). The O···O separations are in the range of 2.55(2)−2.91(1) Å (Supporting Information, Table S3). Such 2D layers are further interlinked into a 3D structure via weak $\pi\cdots\pi$ interactions between neighboring aromatic rings of the bipy ligands (Supporting Information, Table S3, Figure S3).

Magnetic Property Measurements. Temperature-dependent magnetic susceptibility measurements for compounds **1**−**9** and **11** were performed over a temperature range from 2 to 300 K at 1000 Oe. Results from fitting of the susceptibility data according to the Curie−Weiss law are listed in Table 2 along with the measured and expected $\chi_m T$ values.

The temperature dependence of the magnetic susceptibility data of **1** is shown in Figure 8. The $\chi_m T$ value at room

Table 2. Calculated and Measured $\chi_m T$ ($cm^3\ mol^{-1}\ K$) Values at 300 and 2 K, C (Curie Constant) and θ (K) for Compounds **2**−**9** and **11**

compound	$\chi_m T$ (calc)	$\chi_m T$ (300 K)	$\chi_m T$ (2 K)	C	θ/K
2	8.75	8.74	8.26	8.73	−0.54
3	4.375	4.40	4.20	4.38	−0.13
4	8.75	8.92	8.64	8.89	−0.10
5	8.75	8.84	3.93	9.44	−3.33
6	8.75	8.74	1.80	8.84	−4.67
7	8.75	8.78	6.16	8.79	−0.56
8	8.75	8.93	6.34	8.91	−0.99
9	8.75	8.80	5.63	8.82	−0.48
11	4.375	4.51	0.88	4.56	−5.34

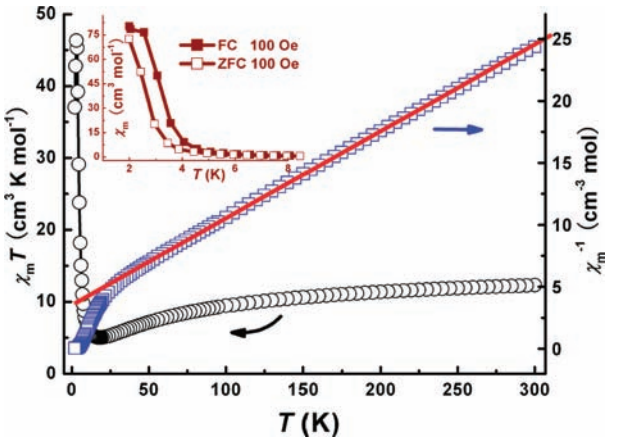

Figure 8. Temperature dependence of $\chi_m T$ and χ_m^{-1} for **1** at $H = 1$ kOe from 2 to 300 K. The solid line is the best-fit according to Curie−Weiss law. Inset: ZFC and FC curves at $H = 100$ Oe from 2 to 10 K.

temperature is 12.31 $cm^3\ mol^{-1}\ K$, which is slightly smaller than the spin-only value expected for three isolated Mn^{2+} ions (13.125 $cm^3\ mol^{-1}\ K$ with $S = 5/2$) per formula unit. As the temperature is lowered, $\chi_m T$ first decreases gradually to a minimum of 5.01 $cm^3\ mol^{-1}\ K$ at 18.4 K, then increases sharply to 46.32 $cm^3\ mol^{-1}\ K$ at about 3.0 K, and finally drops rapidly upon further cooling, probably because of the saturation effect. Fitting of the data above 30 K with the Curie−Weiss law gave $C = 14.28\ cm^3\ mol^{-1}\ K$ and $\theta = -50.7$ K. The negative value of θ and the initial decrease of $\chi_m T$ should be due to the overall antiferromagnetic coupling between the Mn^{2+} ions. The steep rise in $\chi_m T$ at low temperature indicates that a mechanism of ferromagnetic-like correlations exists and develops into a long-range ordering. The shape of the $\chi_m T$ versus T plot, with its (shallow) minimum, is typical of ferrimagnetic behavior or spin canting.

The low-temperature magnetic phenomena ($T < 10$ K) for **1** were scrutinized by applying various magnetic fields. As depicted in Supporting Information, Figure S4, the susceptibility below 5 K is rather field-dependent, indicative of the onset of a ferromagnetic phase transition. The magnetic phase transition is further verified by the divergence in the ZFC-FC magnetization under a small field and the cuspate frequency-independent peaks at about 2.8 K in χ_m' and 2.2 K in χ_m'' of the alternating current (ac) magnetic susceptibility (Figure 9, inset), suggesting a negligible contribution of spin-glass character.

The field dependence of the magnetization, $M(H)$ at 2 K (Figure 9) sharply increases and reach a value of about 3.16 Nβ at a field of 300 Oe, then slowly increases to

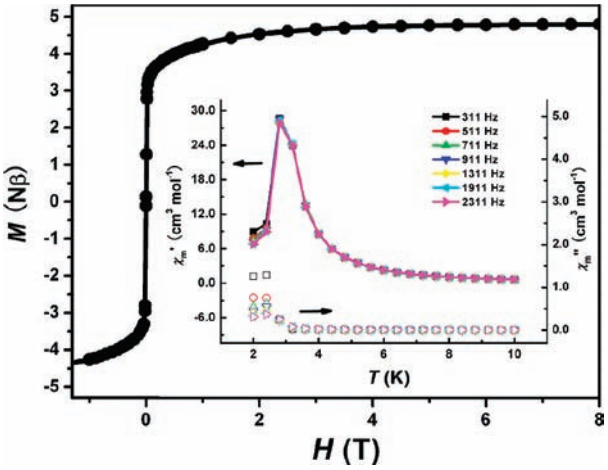

Figure 9. Field dependent isothermal magnetization for **1** at 1.8 K in the ± 8 T range. Inset: the in-phase χ_m' and out-of-phase χ_m'' components of the ac susceptibility of **1** measured at different frequencies (311, 511, 711, 911, 1311, 1911, 2311 Hz) in an applied ac field of 3 Oe.

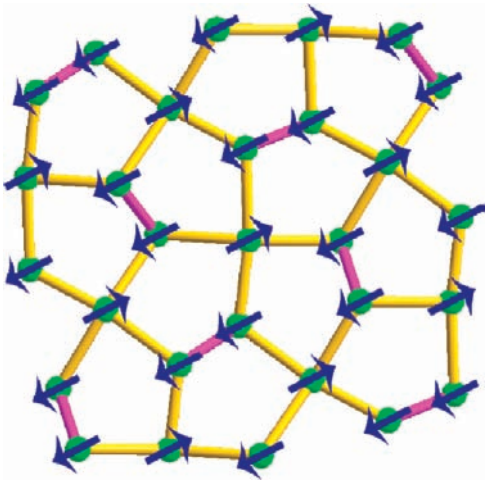

Figure 10. Proposed spin configuration of the (5, $^3/_4$)-topological layer for **1** if only the single oxygen bridge is considered. The blue arrows represent individual moments of spin carriers.

a saturation value of 4.80 Nβ at 80 kOe, which is in accordance with the value anticipated for a net spin value of $S = 5/2$ with $g = 2.0$ (5.00 Nβ) in the ferrimagnetic [5/2 + 5/2−5/2] system. Yet no hysteresis loop was observed at that temperature, as frequently observed in ferrimagnetic molecular systems,[22c] suggesting that compound **1** is a soft ferrimagnet.

Considering the two-dimensional (2D) spin topology that contains congruent pentagons (pentagonal tilting) being similar to the semiregular (5, $^3/_4$)-network illustrated in Figure 10, **1** is an unusual example of homospin ferrimagnet. The main superexchange pathway present in **1** is the single oxygen bridge, and the magnetic coupling through the O−S(or As)−O bridge should be weak (as expected in **2**−**9** and **11** referred infra). From the magnetic point of view, such periodic tilting of pentagons (odd-sided polyhedron) may achieve the non-compensation in spin moments of Mn^{2+} atoms, thereby showing ferrimagnetism. On the other hand, **1** can also be seen as two lattices, one formed by Mn(1) and Mn(2) ions and the other by the Mn(3) ions in a 2:1 ratio. The coupling

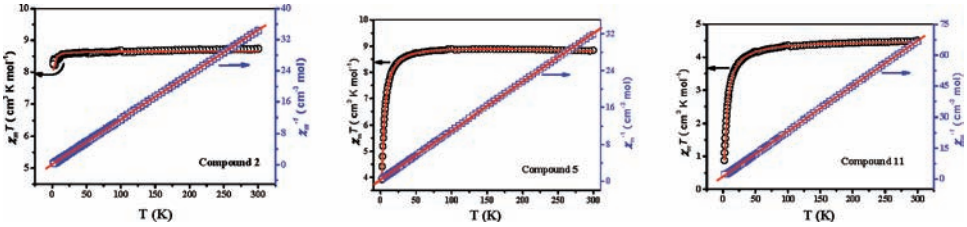

Figure 11. Plots of the $\chi_m T$ product and χ_m^{-1} versus T for **2**, **5**, and **11**. The solid lines represent the best fit to the corresponding classical model and Curie−Weiss law.

between two neighboring Mn(1) or Mn(2) and their own bridged by a pair of single oxygen is expected to be ferromagnetic because of small Mn−O−Mn angles (100.2(2)−101.6(2)°).[22] The ferromagnetically coupled Mn(1) or Mn(2) dimer is antiferromagnetically coupled with neighboring Mn(3) ions because of the much large Mn−O−Mn angles (126.2(2)−130.6(2)°).[26] The antiferromagnetic coupling between the two lattices resulted in an uncompensated spin $S = 5/2$ per every three Mn^{2+} atoms. This corresponds to the ferrimagnetic character of **1**, otherwise frustration or ferromagnetism would be expected. However, it is only a proposed model (Supporting Information, Figure S5), and the real magnetic structure needs to be further analyzed by neutron diffraction. Meanwhile, it is also very difficult to calculate theoretically the magnitude of the coupling constant in such irregular 2D networks of **1**.

Compounds **2**, **3**, and **4** with isolated mononuclear clusters display a similar weakly antiferromagnetic behavior. Their $\chi_m T$ values remain almost unchanged upon cooling (Figure 11 for **2**, Supporting Information, Figure S6 for **3** and **4**). The values of C are in good agreement with the ones expected for two or one magnetically isolated Mn^{2+} ion with $S = 5/2$ per formula unit (8.75 cm^3 K mol^{-1} for **2**, **4** and 4.375 cm^3 K mol^{-1} for **3**). The Weiss constants for **3** and **4** are very close to zero; hence, they are essentially paramagnetic. Magnetic interactions between these mononuclear units are expected to be negligible because they are well separated as discussed in crystal structure sections.

Compound **5** contains two different Mn_2 dimers in which the two manganese(II) ions are interconnected via two Mn−O−As−O−Mn bridges with Mn···Mn separation of 4.0611(9) Å or via a pair of oxygen atoms with Mn···Mn separation of 3.4659(8) Å. Compounds **6**−**9** contain a Mn_2 dimer in which each pair of manganese(II) ions is linked via a single Mn−O−As−O−Mn bridge with much larger Mn···Mn separations than those in **5** (6.624(1) Å for **6**, 5.547(2) Å for **7**, 5.830(2) Å for **8** and 5.205(1) Å for **9**). These compounds exhibit similar magnetic behavior. Their $\chi_m T$ values decrease slightly in most of the temperature range, but decrease more rapidly under very low temperature, indicating weak antiferromagnetic interactions between the two metal centers within the dimer. Fitting of the data according to Curie−Weiss law gives Weiss constants of −3.3(2), −4.7(2), −0.6(1), −1.0(1), and −0.5(1) K for **5**−**9**, respectively (Table 2, Figure 11 for **5**, Supporting Information, Figure S6 for **6**−**9**). The C values obtained are in good agreement with that expected for two or one magnetically isolated Mn^{2+} ions with $S = 5/2$ per formula unit (8.75 cm^3 K mol^{-1} for **5**−**9**). The variable-temperature magnetic susceptibility data of the Mn^{2+} dimers for compounds **5**−**9** were fitted according to the Hamiltonian $H = -2JS_1 \cdot S_2$ with $S_1 = S_2 = 5/2$ as given in the equation.[22a] Fitting of magnetic data gives a satisfactory result with the superexchange parameters of $J_1/k_B = -0.12$ K (for Mn_2 dimer with two Mn−O−As−O−Mn bridges), $J_2/k_B = -0.56$ K (for Mn_2 dimer with two Mn−O−Mn bridges) for **5**, $J/k_B = -0.49$ K for **6**, 0.06 K for **7**, 0.09 K for **8**, and 0.20 K for **9** and $g = 2.04$ for **5**, 2.00 for **6**, 2.01 for **7**, 2.00 for **8**, and 2.01 for **9**. The obtained J values are rather small, indicating that the exchange interactions between the two magnetic centers within the dimers are very weak. These values are also generally smaller than those for manganese(II) phosphonates with similar dinuclear units, indicate that the magnetic exchange through arsonate group is not as efficient as the phosphonate group, probably because of a longer As−O distance than the P−O one.[20c,26]

The magnetic behavior of the compound **11** is approximated by the contributions of Mn^{2+} infinite-regular chain model of classical spins derived by Fisher with $H = -J\Sigma S_i \cdot S_{i+1}$.[22] Fitting of magnetic data using the infinite-regular chain model led to the superexchange parameters of $J_1/k_B = -0.68$ K, $zJ/k_B = -0.005$ K, and $g = 2.03$. The agreement factor defined by $R = \sum(\chi_m T_{exp} - \chi_m T_{cal})^2/\sum(\chi_m T_{exp})^2$ is equal to 1.95×10^{-7}. Fitting of the susceptibility data according to the Curie−Weiss law gives a Curie constant (C) of 4.56 cm^3 K mol^{-1} and a negative Weiss constant ($\theta = -5.3(2)$ K) for **11** (Table 2, Figure 11). These values confirm the presence of very weak intrachain magnetic interaction between the Mn^{2+} ions within the 1D chain, which is probably due to the large separations (6.220 (1) Å) between neighboring magnetic centers (Figure 7). The interchain magnetic interaction is expected to be almost negligible.

It is unfortunate that we could not isolate enough samples for the heptanuclear cluster **10** which might display interesting magnetic properties.

TGA Studies. Thermogravimetric analysis (TGA) curves of compound **1** show two main steps of weight losses (Supporting Information, Figure S7). The first step (111−260 °C) corresponds to the release of one lattice water molecule and three aqua ligands; the observed weight loss of 9.44% is very close to the calculated value (9.06%). The second step covering a temperature range of

(26) (a) Fuller, A. L.; Watkins, R. W.; Dunbar, K. R.; Prosvirin, A. V.; Arif, A. M.; Berreau, L. M. *Dalton Trans.* **2005**, 1891–1896. (b) Ishida, T.; Kawakami, T.; Mitsubori, S.-i.; Nogami, T.; Yamaguchi, K.; Iwamura, H. *J. Chem. Soc., Dalton Trans.* **2002**, 3177–3186. (c) Durot, S.; Policar, C.; Pelosi, G.; Bisceglie, F.; Mallah, T.; Mahy, J.-P. *Inorg. Chem.* **2003**, *42*, 8072–8080. (d) Mukherjee, P. S.; Konar, S.; Zangrando, E.; Mallah, T.; Ribas, J.; Chaudhuri, N. R. *Inorg. Chem.* **2003**, *42*, 2695–2703.

420−650 °C corresponds to the combustion of sulfophenylarsonic ligands. The total weight loss at 650 °C is 46.5%.

TGA curves of compound **2** exhibit two main steps of weight losses (Supporting Information, Figure S7). The first step (83−120 °C) corresponds to the release of 8.5 lattice water molecules; the observed weight loss of 7.5% is close to the calculated values (9.9%). The second step (120−652 °C) corresponds to the combustion of sulfonate-arsonate ligands and phen ligands. The total observed weight losses are 84% at 652 °C for **2**.

TGA curves of compounds **3** and **11** also display two main steps of weight losses (Supporting Information, Figure S7). The first step (91−124 °C for **3** and 71−128 °C for **11**) corresponds to the release of two lattice water molecules, the observed weight losses (5.04% for **3** and 4.9% for **11**) are close to the calculated values (4.8% for **3** and 5.04% for **11**). The second step (233−657 °C for **3** and 260−640 °C for **11**) corresponds to the release of the aqua ligand and the decomposition of the sulfonate-arsonate ligand and phen or bipy auxiliary ligands. The total observed weight losses are 80.3% at 657 °C for **3**, 73.3% at 640 °C for **11**, respectively.

TGA curves of **4** exhibit three main steps of weight losses. The first step before 126 °C is associated with the release of three lattice water molecules. The observed weight loss of 3.3% is close to the calculated value (3.7%). The second step (195−364 °C) corresponds to the decomposition of bipy ligands and perchlorate anions. The third step (364−654 °C) overlaps with the second one, during which the sulfonate-arsonate ligands are combusted. The total observed weight loss is 79.0% at 654 °C.

TGA curves of **6** and **7** exhibit two main steps of weight losses. The first step is associated with the release of lattice water molecules and aqua ligands whereas the second steps correspond to the combustion of the sulfonate-arsonate ligands, auxiliary ligands, and perchlorate anions. The total observed weight losses are 84.3% at 731 °C for **6**, and 83.9% at 752 °C for **7**.

Compound **5** is stable up to 273 °C, then it displays two steps of weight losses. The first step (273−324 °C) corresponds to the release of an aqua ligand. The observed weight loss of 1.49% is close to the calculated value (1.53%). The second step corresponds to the combustion of sulfonate-arsonate ligands and phen ligands. The total observed weight loss at 680 °C is 72.9%. Compound **8** is stable before 200 °C, then it displays two continuous steps of weight losses. The first step covering a temperature range of 200−340 °C corresponds to the release of one lattice water molecule and an aqua ligand, as well as the partial combustion of the bipy co-ligands. The second step (340−700 °C) overlaps with the first one, and corresponds to further combustion of the bipy and arsonate ligands. The total weight loss at 700 °C is 74.3%.

Compound **9** is stable up to 370 °C, then it exhibits two continued steps of weight losses, the first one (370−435 °C) is mainly due to the combustion of the terpy ligand and the second one (435−660 °C) is mainly associated with the combustion of sulfonate-arsonate ligands. The total observed weight loss at 660 °C is 74.2%. The final residuals for all compounds were not characterized.

As is shown in Supporting Information, Figure S7, it is noted that the stabilities of **5** and **9** are much higher than that of the remaining compounds because of the lack of intercluster guest molecules.

Conclusions

In summary, by introducing various auxiliary chelating ligands, we have successfully reduced the 2D manganese(II) sulfo-arsenate into various types of low dimensional assemblies including mononuclear, dinuclear, heptanuclear, and 1D structures. These results may provide some insights to the rational design of low dimensional materials. The *o*-sulfophenylarsonic acid is a versatile ligand and is able to adopt many types of coordination modes similar to the corresponding phosphonate ligands. The pK_a value of the phenylphosphonic acid is 1.86, 7.51 and the pK_a value of the phenylarsonic acid is 3.39, 8.25;[27] hence, the phenylarsonate ligand is more likely to be partially protonated and binding with fewer metal centers as compared with the corresponding phosphonic acid.

The factors that affect the types of structures formed are rather complicated and difficult to be summarized. It is noticed, however, that the metal sources, reaction temperatures, molar ratios of the starting materials, pH values of the reaction media, as well as of the auxiliary ligands, all played an important role. It is found that the coordination of an aqua ligand to the metal center will change the coordination mode of the arsonate ligand as in **3**, **6**, and **7** compared to other dinuclear compounds. The presence of a μ_3-hydroxyl anion facilitates the formation of a high nuclear cluster such as heptanuclear **10**. However, much more systematic work is needed to further elucidate the factors that control the structures of the resultant complexes. It is also anticipated that more new types of mutinuclear clusters of other transition metal or lanthanide(III) sulfonate-arsonates can be designed by using such a synthetic route.

Acknowledgment. This work was supported by the National Natural Science Foundation of China (Nos. 20973170 and 20825104), Key Project of Chinese Academy of Sciences (No. KJCX2-YW-H01) and 973 Program (No. 2006CB932903), the major project from FJIRSM (SZD09001).

Supporting Information Available: X-ray crystallographic files in CIF format, tables of selected bond lengths, hydrogen bonds and $\pi\cdots\pi$ interactions, 3D network structures of all compounds, magnetic property pictures of some compounds, TGA diagram, IR spectra, simulated and measured XRD patterns for all compounds. This material is available free of charge via the Internet at http://pubs.acs.org.

(27) (a) Nagarajan, K.; Shelly, K. P.; Perkins, R. P.; Stewart, R. *Can. J. Chem.* **1987**, *65*, 1729–1733. (b) Kina, K.; Tôei, T. *Bull. Chem. Soc. Jpn.* **1971**, *44*, 2416–2419.